DOI: 10.1002/ejic.201000907

Bonding Interactions between Nitrous Oxide (N_2O) and Mono-Ruthenium Substituted Keggin-Type Polyoxometalates: Electronic Structures of Ruthenium/N_2O Adducts

Chun-Guang Liu,[a,b] Wei Guan,[a] Li-Kai Yan,[a] and Zhong-Min Su*[a]

Keywords: Polyoxometalates / Ruthenium / Nitrous oxide / Bonding interactions / Density functional calculations

Density functional theory (DFT) calculations were performed for three ruthenium/nitrous oxide(N_2O) adducts, $Ru^{II}Cl_2(\eta^1\text{-}N_2O)(P\text{–}N)(PPh_3)$ {P–N = [*o*-(dimethylamino)phenyl]diphenylphosphane} (**1**), $Ru^{II}(\eta^1\text{-}N_2O)(TMP)(THF)$ (TMP = dianion of tetramesitylporphyrin, THF = tetrahydrofuran) (**2**), and $[PW_{11}O_{39}\{Ru^{II}/(\eta^1\text{-}N_2O/H_2O)\}]^{n-}$ (**3**). The bonding interactions between the N_2O molecule and the metal–ruthenium fragment were determined from the energy-decomposition analysis (EDA) and their electronic structures. The results show that the bonding in the ruthenium(II)/N_2O adducts **1**–**3** can be interpreted in terms of weak donor–acceptor interactions between the N_2O molecule and the ruthenium(II) center. The geometrical optimization of the polyoxometalate (POM) adduct **3** indicates a bent Ru–NNO linkage, which effectively enhances donor–acceptor interactions with the quasi π-symmetry orbital. The mono-ruthenium(II) substituted Keggin-type POM adduct **3** is a potential reagent for the activation of the N_2O molecule because of the strong Ru–NNO bond and the significant RuNN–O π^*-antibonding orbital character relative to adducts **1** and **2**, according to our DFT calculations.

Introduction

Nitrous oxide (N_2O) is a potential greenhouse gas;[1] it can affect the atmospheric ozone concentration. The efficient removal or conversion of N_2O has attracted considerable attention. Chemistry and catalysis relevant to the control of N_2O emissions are focused on the activation of N_2O by transition-metal complexes. Although a large number of reactions between transition-metal complexes and N_2O have been reported based on experimental and theoretical studies, it is always regarded as a kinetically inert molecule and very poor ligand.[2] Thus, none of the crystallographic structures of metal complexes containing the N_2O ligand are reported.

Various reactions between metal complexes and the N_2O molecule, including cleavage of N_2O to give terminal/bridged metal-oxide/oxido complexes, insertion of the N_2O oxygen atom into M–C and M–H bonds, and oxidation of CO/PR_3 ligands of metal complexes, have been explored.[3] Among them, the utilization of the N_2O molecule as an oxygen donor in the synthesis is receiving increasing attention because of the high O components of the N_2O molecule and the environmentally benign byproduct N_2. To date, the mechanisms of these reactions are unclear because it is difficult to detect N_2O complexes. But coordination of N_2O to form the metal/N_2O adduct is the key step in the reaction of oxygen transfer from N_2O to alkyl, alkene, and imido ligands, etc. Armor and Taube have spectroscopically characterized the structure of the metal/N_2O adduct,[4] $[Ru^{II}(NH_3)_5(N_2O)]^{2+}$, where the ruthenium(II) atom coordinates to the terminal N atom of the N_2O molecule in a linear end-on mode. As another rare example, the metal/N_2O adduct, $Ru^{II}Cl_2(\eta^1\text{-}N_2O)(P\text{–}N)(PPh_3)$ {P–N = [*o*-(dimethylamino)-phenyl]diphenylphosphane} (**1**) (see Figure 1) has been characterized by using $^{31}P(^1H)$ NMR spectroscopy.[5] Furthermore, the ^{15}N NMR spectrum confirmed that N_2O is ligated through the terminal nitrogen atom. The experimental measurements showed that it is stable below –40 °C. Another interesting example is the catalyzed oxidation of the organic substrate with N_2O by a ruthenium porphyrin,[6] $Ru^{II}(TMP)(THF)$ (TMP = dianion of tetramesitylporphyrin, THF = tetrahydrofuran). Treatment of it and N_2O in the toluene solution gave the ruthenium porphyrin dioxido species, $Ru^{VI}(TMP)(O)_2$, which displayed high reactivity in the oxygen-transfer reaction. ^1H NMR spectra suggested that reaction intermediates should contain a ruthenium porphyrin/N_2O adduct, $Ru^{II}(TMP)(THF)(N_2O)$ (**2**) (see Figure 1). These results show that the ruthenium atom is unique relative to other metal atoms, and it may serve as a good activation center for the inert N_2O molecule.

Polyoxometalates (POMs) are early transition-metal oxido clusters; this class of inorganic compounds is unmatched not only in terms of molecular structural diversity but also with regard to reactivity and relevance to analytical

[a] Institute of Functional Material Chemistry, Faculty of Chemistry, Northeast Normal University, Changchun 130024, P. R. China
[b] College of Chemical Engineering, Northeast Dianli University, Jilin City 132012, P. R. China
Fax: +86-0431-85684009
E-mail: zmsu@nenu.edu.cn

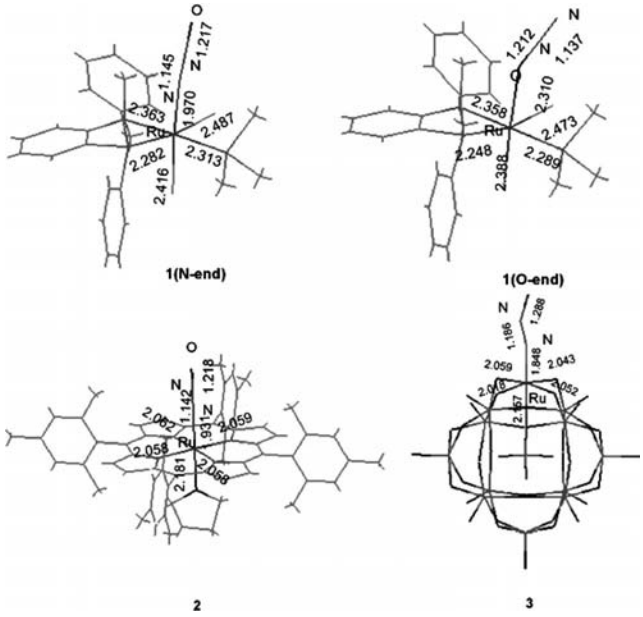

Figure 1. Optimized geometries (bond lengths [Å]) at the BP86/TZP calculations of all the ruthenium(II) adducts studied here.

chemistry, catalysis, medicine, and materials science.[7] In the past decade reactions of POM adducts with N_2O have been reported, most of them focus on transition-metal substituted POMs.[8] Neumann et al. described the activation of N_2O by a sandwich-type Mn^{III}-substituted POM, $Q_{10}[Mn^{III}_2ZnW(ZnW_9O_{34})_2]$ [Q = $(C_8H_{17})_3CH_3N^+$] to epoxidation of alkenes,[8a] and a divanadium-substituted Keggin-type POM [$\{n\text{Bu}_4\text{N}\}_5\{PV_2Mo_{10}O_{10}\}$] to oxidize alcohols and alkylarenes.[8b] On the basis of experimental observations, they showed that reaction mechanisms are different from each other, but that the electron-transfer features between the POM complex and N_2O in the POM/N_2O adduct is very important for the activation of the N_2O molecule.

On the basis of the good nature of the ruthenium atom for activation of N_2O in the ruthenium(II) porphyrin and relevant ruthenium(II) complexes,[5,6] the mono-ruthenium substituted Keggin-type POM should thus be considered for the activation of N_2O because it possesses an analogous coordination sphere to the metalloporphyrin, and its catalytic feature is similar to that observed for metalloporphyrins in oxygen-transfer reactions.[9] The low-valent ruthenium(II) derivative of the Keggin-type POM has been reported,[10] the ruthenium(II) center is replaced by a tungsten- or molybdenum-oxido group at the Keggin-typical POM surface. The lacunary POM ligand represents a bonding site that is pentadentate, and thus the octahedral coordination sphere of the ruthenium(II) center needs to be completed by an additional sixth labile ligand, H_2O, which generates Keggin-type aquametal derivatives (**I**) (see Figure 2).[11]

The reaction intermediates are very difficult to isolate and characterize experimentally. By contrast, the quantum chemical calculation based on the density functional theory

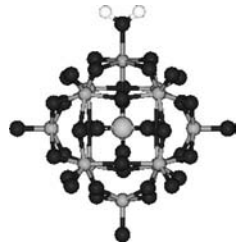

Figure 2. The ball and stick model of the mono-ruthenium substituted Keggin-type polyoxometalate $[\{PW_{11}O_{39}\}Ru^{II}(H_2O)]^{5-}$ (**I**).

(DFT) is a useful tool for understanding and rationalizing the electronic structure and reactivity of the transition-metal-substituted Keggin-type POM and analogous metal complexes.[9g,12] In this paper we report on a detailed DFT calculation for mono-ruthenium substituted Keggin-type POMs. The aim of this work is to look at the electronic structures of the N_2O/POM adduct and bonding features between the ruthenium center and the N_2O molecule.

Results and Discussion

1. Why Does the N_2O Molecule Coordinate to the Ruthenium(II) Center with the Terminal Nitrogen Atom?

The ground-state geometries of the adduct **1** optimized by BP86/TZP calculations are shown in Figure 1. It should be stressed that the phenyl ring of the triphenylphosphane ligand has been simplified to a methyl group in order to save on computational costs. The N_2O molecule can coordinate to the metal center through the O end or N end. In this paper both of the possible models have been considered for adduct **1**. The BP86/TZP calculations show that the N-end coordination model is 15.69 kcal mol^{-1} more stable than that of the O-end coordination model for adduct **1**, which is in good agreement with the experimental result.[5] DFT calculations show that the two bonding models give very different structures, the RuNNO unit displays slight bending character [171.59° for RuNN(O) angle] for the N-end coordination model, whereas the bonding with the terminal oxygen atom gives a more bent structure [the calculated RuON(N) angle is 127.37°] (see Figure 1). This feature has also been found for another ruthenium adduct, $[Ru^{II}(NH_3)_5(N_2O)]^{2+}$, based on DFT calculations using different levels of theory.[18] The calculated Ru–NNO bond length (1.97 Å) in the N-end model is shorter than the Ru–ONN bond length (2.31 Å) in the O-end model, Δr(Ru–N/Ru–O) = 0.3 Å.

The data in Table 1 show that the interaction energy between the N_2O molecule and the metal fragment in the N-end model (–21.05 kcal mol^{-1} for Ru–NNO bond) is significantly larger than the interaction energy of the Ru–ONN bond in the O-end model (–2.61 kcal mol^{-1}). We note that the contribution of electrostatic attractions ΔE_{elstat} of the Ru–ONN bond in the O-end model is greater than the orbital interaction, and displays high ionic character, while for the N-end model, the orbital interaction ΔE_{orb} and elec-

trostatic attractions are nearly the same for the Ru–NNO bond. This indicates that the Ru–NNO bond in the N-end model has a higher degree of covalent bonding (49.5%) than the Ru–ONN bond in the O-end model (39%).

Table 1. Energy decomposition analysis of all the ruthenium(II) adducts at the BP86/TZP calculations (energy contributions for Ru^{II}–NNO or Ru^{II}–ONN bond in kcal mol^{-1}).

	1(η^1-N)	**1**(η^1-O)	**2**	**3**	**I**
ΔE_{int}	–21.05	–2.61	–28.08	–76.81	–23.17
ΔE_{Pauli}	112.65	43.82	109.34	142.67	69.77
ΔE_{elsat}	–67.57	–28.23	–64.63	–85.84	–62.15
ΔE_{orb}	–66.13	–18.20	–72.79	–133.64	–30.79
ΔE_{prep}	13.52	–	5.57	30.64	2.49
$\Delta E_{prep}(Ru^{II})$	13.17	–	5.29	6.24	1.74
$\Delta E_{prep}(H_2O/N_2O)$	0.35	–	0.28	24.4	0.75
ΔE (= $-D_e$)	–7.53	–	–22.51	–46.17	–20.68

The ruthenium(II) center in adduct **1** possesses a d^6 electronic configuration with low spin, which leads to the t_{2g} orbitals d_{xy}, d_{xz}, and d_{yz} being fully occupied. As a result they can only serve as a π-donation orbital and not a π-acceptor orbital (see Figure 3). Figure 4 shows the molecular orbital diagram for free N_2O, the two σ orbitals are easily identified, and display lone pair character on the terminal oxygen and nitrogen atoms, and thus they can serve as both an O- and N-donation orbital with σ symmetry, and provide a good orbital basis for O-end- and N-end-coordinated models. The N-donation orbital is ca. 3.5 eV higher in energy than that of the O-donation orbital according to BP86/TZP calculations. The large energetic difference between the low-lying, σ-donation orbital of the N_2O molecule and the high-energy, unoccupied metal d_{z^2} orbital is a key unmatched factor for the bonding interaction between two fragments. Thus, the more low-lying O-donation orbital of the N_2O molecule would be more unmatched than the N-donation orbital for the donor–acceptor bonding interaction with σ symmetry, which does not favor the O-end-coordinated model for adduct **1** (see Figure 3). The EDAs also support the evidence that the Ru–ONN bond has a low orbital interaction energy, and displays high ionic character. Because the bonding contribution of electrostatic attractions ΔE_{elstat} to the Ru–ONN bond has been largely cancelled by the repulsive term ΔE_{Pauli}, the interaction energy between the N_2O molecule and the metal fragment of the O-end model is very small –2.61 kcal mol^{-1} (see Table 1). For the porphyrin and POM adducts, **2** and **3**, respectively, the optimized calculations can not give the O-end-coordinated model because of the very weak bonding interaction.

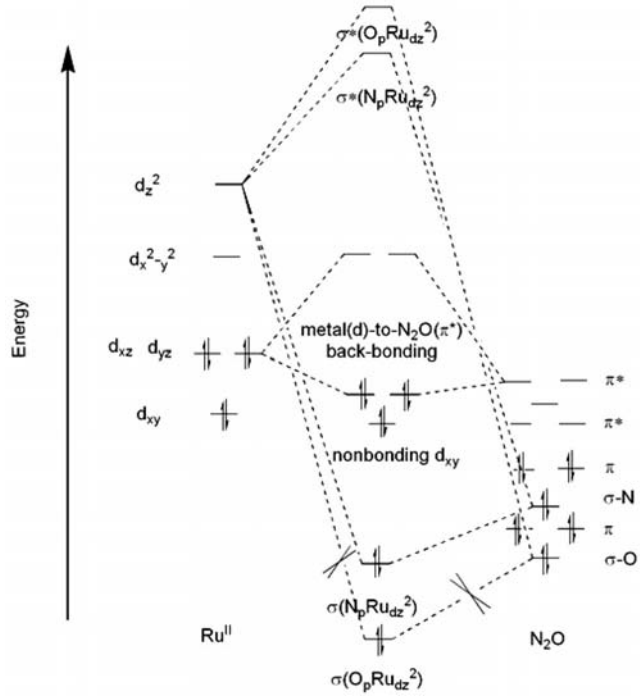

Figure 3. Schematic representation of the σ(Ru–NNO/Ru–ONN) and metal(d)-to-$N_2O(\pi^*)$ back-bonding interaction in the linear end-on mode.

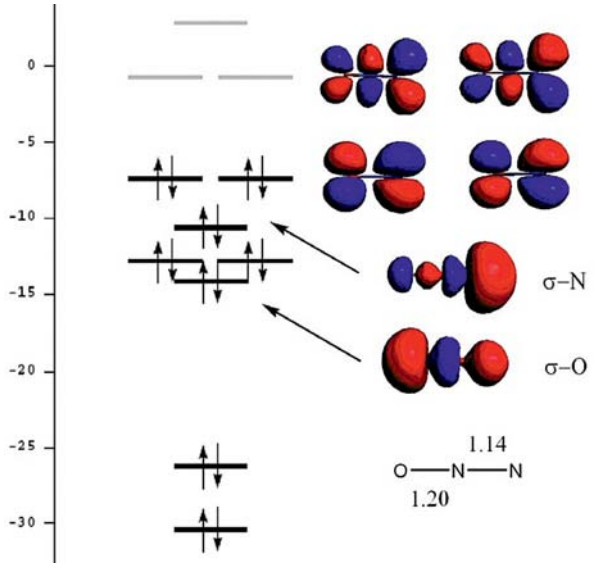

Figure 4. Molecular orbital diagram for free N_2O obtained by BP86/TZP calculations, energies are given in eV.

2. Is It Possible for the POM Adduct 3 to Activate the N_2O Molecule?

Porphyrin and lacunary POM ligands have analogous bonding situations to that of the ruthenium(II) center. Moreover, the porphyrin complex has been used to prepare a high-valent ruthenium-dioxido species by the activation of the N_2O molecule.[5] Figure 1 shows the optimized geometries of the porphyrin and POM adducts, **2** and **3**, respectively. It is very necessary to analyze the geometrical data in detail because the calculated results already provide valuable information about the bonding features of the molecule. The BP86/TZP calculated bond angles of the RuNN(O) and (Ru)NNO units (165.17 and 143.0°) are more bent in POM adduct **3** than the porphyrin adduct **2** that has a nearly linear model. The calculated value for the Ru–NNO bond length of the POM adduct **3** (1.848 Å) is smaller than that determined for the other two adducts **1**

and **2** (1.970 and 1.931 Å). This suggests that the POM adduct **3** possesses a strong Ru–NNO bond relative to adducts **1** and **2**. The theoretical BDEs of all ruthenium(II) adducts at the BP86/TZP levels also indicate that the POM adduct **3** has a much stronger Ru–NNO bond (D_e = 46.17 kcal mol^{-1}) than adducts **1** and **2** (D_e = 7.53 and 22.51 kcal mol^{-1}, respectively) (see Table 1). Generally, the low-valent aquametal derivative of the Keggin-type POM complex contains a water molecule coordinated to the metal center (see Figure 2). Thus, the activation of the N_2O molecule by the ruthenium(II) center needs to replace the aqua ligand with the N_2O molecule. The BP86/TZP results suggest that substitution of the aqua ligand of the POM complex **I** by the N_2O molecule gives a larger total bond energy in the POM adduct **3** (D_e = 46.17 kcal mol^{-1}) than in **I** (D_e = 20.68 kcal mol^{-1}) (see Table 1).

The enhancement of the Ru–NNO bonding interaction in the POM adduct **3** is mainly due to the large orbital interaction energy ΔE_{orb}; it is about twice as large as that of adducts **1** and **2** (see Table 1). Figure 5 shows the frontier molecular orbital (FMO) of all adducts. We are now only concerned with the shape of the HOMO–2 of the POM adduct **3**, it clearly reveals the metal-based d_{yz} orbital character, and some contributions at the N_2O molecule. The bent structure of the RuNNO unit provides a very specific topology for this orbital, it enhances the Ru–NNO bonding interaction by a quasi Ru–NNO π-bonding orbital. This remarkable topology thus explains the large orbital interaction energy for the Ru–NNO bond of the POM adduct **3**.

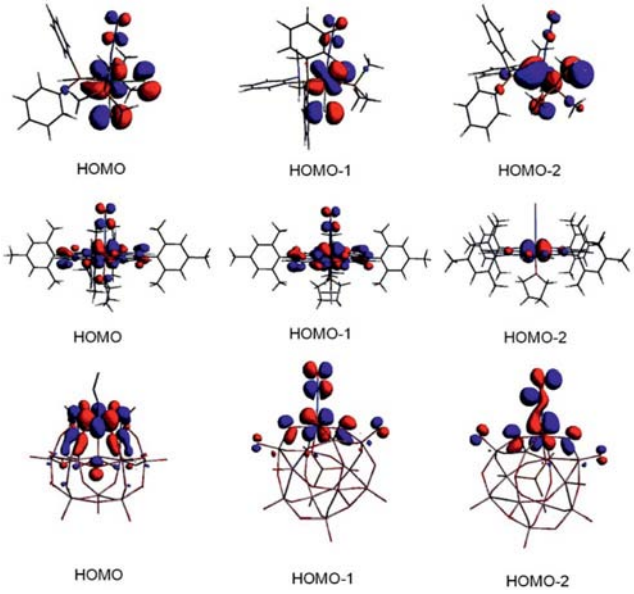

Figure 5. The metal-based t_{2g} orbitals of all ruthenium(II) adducts studied here.

Activation of N_2O as an O donor is a result of the cleavage of the RuNN–O bond. The optimized calculations show that the RuNN–O bond length increases in the order **1** < **2** < **3**, but these differences are not substantial. All of the RuNN–O bond lengths in these adducts are longer than that in the free N_2O molecule (1.20 Å) according to BP86/TZP calculations (Δr = 0.02–0.09 Å) (see Figure 1). A large number of experimental and theoretical studies have suggested that N_2O was activated by accepting two electrons from the metal center.[2a,2b,3f,3k,3l] Thus, the fully occupied t_{2g} orbitals of the ruthenium(II) center, d_{xy}, d_{xz}, and d_{yz}, with potential π-donation orbital character become very important for activation of the N_2O molecule. The FMOs of adduct **1**, **2**, and **3** are shown in Figure 4, while Table 2 summarizes the electronic structural parameters. It can be found that the HOMO, HOMO–1, and HOMO–2 of these adducts are the metal-based t_{2g} orbitals. Compared with adducts **1** and **2**, the metal-based d_{xy} orbital (HOMO) of the POM adduct **3** causes a rearrangement of the orbital order. This arises from the geometrical differences of the first coordination sphere of the ruthenium(II) center among the three adducts. For adducts **1** and **2**, the four coordinated atoms of the equatorial site are nearly coplanar, by contrast, the ruthenium(II) center is pushed out of the equatorial plane with respect to the four coordinated oxygen atoms in the POM adduct **3**, and thus the ruthenium atom hangs over the plane. This effect increases the amount of POM ligand character in the metal-based d_{xy} orbital, and displays some antibonding features between the ruthenium(II) center and four coordinated oxygen atoms, which raises its energy, reflecting the HOMO of the adduct **3**. Because of symmetry forbidden transitions, the metal-based d_{xy} orbital in these adducts can not serve as a π-donation orbital. The metal-based d_{xy} orbital (HOMO–2) of adduct **1** contains the contributions from the (RuN)NO unit because of the broken symmetry caused by the mixing of the metal-based d_{xy} orbital and the p orbital of the chlorine atom, but the relevant low compositions on the (RuN)NO unit indicate that it is not a strong π-donation orbital.

Table 2. Electronic structure parameters for all ruthenium(II) adducts studied here (molecular orbital compositions [%]).

Orbital	**1**				**2**				**3**			
	Ru	N	N	O	Ru	N	N	O	Ru	N	N	O
HOMO–2	54	0	0	0	88	0	0	0	38	3	12	17
HOMO–1	54	0	3	4	49	0	4	5	55	0	7	11
HOMO	53	0	4	5	50	0	4	5	55	0	0	0

The HOMO and HOMO–1 of adducts **1** and **2**, and HOMO–1 and HOMO–2 of adduct **3** are the metal-based d_{xz} and d_{yz} orbitals, respectively. These orbitals are mainly localized on the ruthenium(II) center and the (RuN)NO unit of the N_2O molecule, displaying the metal(d)-to-$N_2O(\pi^*)$ back-bonding interaction. These orbitals may be viewed as RuNN–O π*-antibonding orbitals. Because of the antibonding features of these occupied orbitals, the RuNN–O bond length in all adducts is longer than that of the free N_2O molecule. For the POM adduct **3**, the contributions of the (RuN)NO unit in HOMO–1 and HOMO–2 are 18% and 29%, respectively, which is larger than that of the (RuN)NO unit in HOMO and HOMO–1 for adducts **1** and **2** (ca. 9%) (see Table 2). The high compositions of the (RuN)NO unit in the two orbitals of the adduct **3** effectively enhance the RuNN–O π*-antibonding character.

As an oxygen donor in synthesis, the attack of the oxygen atom of the N_2O molecule is thus important in many of the catalytic processes. Thus, the reactivity of the adducts studied here is usually associated with the acidity/basicity of the oxygen sites. In this paper, we employed a molecular electrostatic potential (MEP), which plots an electrostatic potential (EP) over an electron density isosurface to describe the basicity of the molecules. The EP values at each point are coded by colors. Red-yellow indicates the nucleophilic regions and green-blue the electrophilic regions. As shown in Figure 6, the MPE analysis predicts that the oxygen atom of the N_2O molecule in all ruthenium(II) adducts studied here is basic (red area in Figure 6), but it is not the most basic site in the whole molecule. The chlorine atom in the adduct **1**, the oxygen atom of the THF ligand in the adduct **2**, and oxygen atoms of the POM ligand in the adduct **3** are more basic than the oxygen atom of the N_2O molecule. Especially for the POM adduct **3**, which is stable under the acidic conditions and has protons that are stabilized by an attractive interaction with more negative EP (printed in red) regions, the MPE analysis suggests that the protonated site is likely to be the more basic oxygen atoms of the lacunary POM ligand, and not the oxygen atom of the N_2O molecule. This suggests that the oxygen atom of the N_2O molecule is not occupied by protons that are available for the oxygen-transfer reaction. The ruthenium(II) center in each adduct is identified in green because of its cationic character.

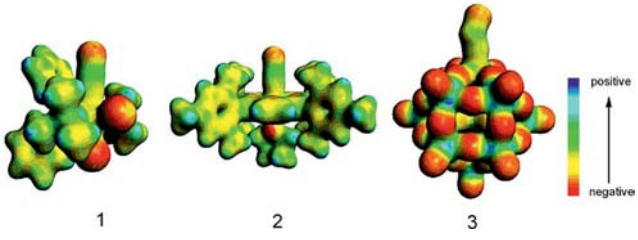

Figure 6. MEP for all ruthenium(II) adducts studied here. The more nucleophilic regions are printed in red, green and blue denotes the less nucleophilic regions.

On the basis of the above mentioned, we theoretically conclude that the mono-ruthenium(II) substituted Keggin-type POM can serve as a potential reagent for the activation of the N_2O molecule because of the strong Ru–NNO bond and significantly RuNN–O π*-antibonding orbitals relative to adducts **1** and **2** that have been used to activate N_2O experimentally.

Conclusions

The theoretical data present here suggest that the bonding interactions between the N_2O molecule and the ruthenium(II) center in adducts **1**–**3** can be referred to as weak donor–acceptor interactions. A detailed comparison of the O-end and N-end models for the N_2O molecule coordination to the ruthenium(II) center in adduct **1** indicates that the O-end model is unstable. The bending structure of the RuNNO unit provides a quasi Ru–NNO π-bonding orbital and effectively enhances the Ru–NNO bond of POM adduct **3**. The mono-ruthenium(II)-substituted Keggin-type POM adduct **3** can serve as a potential reagent for the activation of the N_2O molecule because of the strong Ru–NNO bond and significantly RuNN–O π*-antibonding orbitals relative to adducts **1** and **2**, according to our DFT calculations.

Computational Details

BP86 generalized gradient approximations[13] and VWN[14] local density functionals have been employed for the consideration of the exchange-correlation effect. Triple-ζ basis plus polarization Slater-type orbital basis sets (TZP), and integration parameter 6.0, as implemented in the ADF 2008 program system.[15] The 1s shell for C, N, O, 1s to 2p shells for P, Cl, 1s to 3d shells for Ru, and 1s to 4d shells for W have been treated by frozen core approximations. The relativistic effects were taken into account by using the zero-order regular approximation (ZORA).[16]

The energy-decomposition analysis (EDA)[17] has been employed to investigate interactions between the ruthenium(II) center and the N_2O ligand. There are several contributions to the bond dissociation energy D_e (by definition with opposite sign to ΔE) with physically meaningful entities. Firstly, the ΔE is separated into two major components ΔE_{prep} and ΔE_{int}.

$$\Delta E = \Delta E_{prep} + \Delta E_{int}$$

The preparation energy ΔE_{prep} represents the relaxation of the fragments into their electronic and geometrical ground states. The instantaneous interaction energy, ΔE_{int}, which represents bonding details between two fragments, can be divided into three main components.

$$\Delta E_{int} = \Delta E_{elstat} + \Delta E_{Pauli} + \Delta E_{orb}$$

Here, ΔE_{elstat} represents the quasi-classical electrostatic interaction between the unperturbed charge distributions of the prepared atom. The Pauli repulsion term ΔE_{Pauli} corresponds to the destabilizing interactions between electrons of the same spin on either fragment. The stabilizing orbital interaction term ΔE_{orb} accounts for charge-transfer and polarization effects.

Acknowledgments

The authors gratefully acknowledge the financial support from the National Natural Science Foundation of China (project number 20971020), Program for Changjiang Scholars and Innovative Research Team in University (IRT0714), Department of Science and Technology of Jilin Province (20082103), the Training Fund of NENU's Scientific Innovation Project (STC07017), and Science Foundation for Young Teachers of Northeast Normal University (20090401). We also thank Yuhe Kan for computational support.

[1] a) R. E. Dickinson, R. J. Cicerone, *Nature* **1986**, *319*, 109–115; b) R. J. Cicerone, *Science* **1987**, *237*, 35–42; c) R. J. Cicerone, *Geophys. Res.* **1989**, *94*, 18265–18271; d) W. C. Trogler, *Coord. Chem. Rev.* **1999**, *187*, 303–327.

[2] a) P. Chen, I. Cabrito, J. J. G. Moura, I. Moura, E. I. Solomon, *J. Am. Chem. Soc.* **2002**, *124*, 10497–10507, and references cited therein; b) H. Z. Yu, G. C. Jia, Z. Y. Lin, *Organometallics* **2009**, *28*, 1158–1164; c) R. R. Conry, J. M. Mayer, *Inorg. Chem.* **1990**,

29, 4862–4867; d) A. W. Kaplan, R. G. Bergman, *Organometallics* **1998**, *17*, 5072–5085.
[3] For example: a) F. Bottomley, D. E. Paez, P. S. White, *J. Am. Chem. Soc.* **1981**, *103*, 5581–5582; b) F. Bottomley, D. E. Paez, P. S. White, *J. Am. Chem. Soc.* **1982**, *104*, 5651–5657; c) M. J. Almond, A. J. Downs, R. N. Perutz, *Inorg. Chem.* **1985**, *24*, 275–281; d) F. Bottomley, G. O. Egharevba, I. J. B. Lin, P. S. White, *Organometallics* **1985**, *4*, 550–553; e) A. R. Chadeayne, P. T. Wolczanski, E. B. Lobkovsky, *Inorg. Chem.* **2004**, *43*, 3421–3432; f) S. I. Gorelsky, S. Ghosh, E. I. Solomon, *J. Am. Chem. Soc.* **2006**, *128*, 278–290; g) F. Rondinelli, N. Russo, M. Toscano, *Inorg. Chem.* **2007**, *46*, 7489–7493; h) K. Fujita, D. M. Dooley, *Inorg. Chem.* **2007**, *46*, 613–615; i) W. H. Harman, C. J. Chang, *J. Am. Chem. Soc.* **2007**, *129*, 15128–15129; j) S. Ghosh, S. I. Gorelsky, S. D. George, J. M. Chan, I. Cabrito, D. M. Dooley, J. J. G. Moura, I. Moura, E. I. Solomon, *J. Am. Chem. Soc.* **2007**, *129*, 3955–3965; k) H. Yu, G. Jia, Z. Lin, *Organometallics* **2007**, *26*, 6769–6777; l) H. Yu, G. Jia, Z. Lin, *Organometallics* **2008**, *27*, 3825–3833; m) E. Otten, R. C. Neu, D. W. Stephan, *J. Am. Chem. Soc.* **2009**, *131*, 9918–9919; n) I. B. Nahum, A. K. Gupta, S. M. Huber, M. Z. Ertem, C. J. Cramer, W. B. Tolman, *J. Am. Chem. Soc.* **2009**, *131*, 2818–2820.
[4] a) J. N. Armor, H. Taube, *J. Am. Chem. Soc.* **1969**, *91*, 6874–6876; b) J. N. T. Armor, *J. Chem. Soc., Chem. Commun.* **1971**, 287–288.
[5] C. B. Pamplin, E. S. F. Ma, N. Safari, S. J. Rettig, B. R. James, *J. Am. Chem. Soc.* **2001**, *123*, 8596–8597.
[6] J. T. Groves, J. S. Roman, *J. Am. Chem. Soc.* **1995**, *117*, 5594–5595.
[7] a) C. L. Hill, *Chem. Rev.* **1998**, *98*, 1–2; b) A. Proust, R. Thouvenot, P. Gouzerh, *Chem. Commun.* **2008**, 1837–1852.
[8] a) R. Ben-Daniel, L. Weiner, R. Neumann, *J. Am. Chem. Soc.* **2002**, *124*, 8788–8789; b) R. Ben-Daniel, R. Neumann, *Angew. Chem. Int. Ed.* **2003**, *42*, 92–95; c) J. Ettedgui, R. Neumann, *J. Am. Chem. Soc.* **2009**, *131*, 4–5.
[9] a) A. M. Khenkin, D. Kumar, S. Shaik, R. Neumann, *J. Am. Chem. Soc.* **2006**, *128*, 15451–15460; b) C. L. Hill, R. B. Brown, *J. Am. Chem. Soc.* **1986**, *108*, 536–538; c) D. Mansuy, J. F. Bartoli, P. Battioni, D. K. Lyon, R. G. Finke, *J. Am. Chem. Soc.* **1991**, *113*, 7222–7226; d) P. T. Meiklejohn, M. T. Pope, R. A. Prados, *J. Am. Chem. Soc.* **1974**, *96*, 6779–6781; e) F. Ortega, M. T. Pope, *Inorg. Chem.* **1984**, *23*, 3292–3297; f) X. Wei, R. E. Bachman, M. T. Pope, *J. Am. Chem. Soc.* **1998**, *120*, 10248–10253; g) S. P. de Visser, D. Kumar, R. Neumann, S. Shaik, *Angew. Chem. Int. Ed.* **2004**, *43*, 5661–5665, and references cited therein.
[10] C. Rong, M. T. Pope, *J. Am. Chem. Soc.* **1992**, *114*, 2932–2938.
[11] a) M. T. Pope, A. Müller, *Angew. Chem. Int. Ed. Engl.* **1991**, *30*, 34–48; b) M. Sadakane, E. Steckhan, *Chem. Rev.* **1998**, *98*, 219–238.
[12] a) S. Romo, N. S. Antonova, J. J. Carbo, J. M. Poblet, *Dalton Trans.* **2008**, 5166–5172; b) C. G. Liu, Z. M. Su, W. Guan, L. K. Yan, *Inorg. Chem.* **2009**, *48*, 541–548; c) C. G. Liu, W. Guan, L. K. Yan, P. Song, Z. M. Su, *Dalton Trans.* **2009**, 6208–6213.
[13] a) A. D. Becke, *Phys. Rev. A* **1988**, *38*, 3098–3100; b) J. P. Perdew, *Phys. Rev. B* **1986**, *33*, 8822–8824.
[14] S. H. Vosko, L. Wilk, M. Nusair, *Can. J. Phys.* **1980**, *58*, 1200–1211.
[15] a) For chemistry with ADF, see: G. Te Velde, F. M. Bickelhaupt, E. J. Baerends, C. Fonseca Guerra, S. J. A. van Gisbergen, J. G. Snijders, T. Ziegler, *J. Comput. Chem.* **2001**, *22*, 931–967; b) C. Fonseca Guerra, J. G. Snijders, G. te Velde, E. J. Baerends, *Theor. Chem. Acc.* **1998**, *99*, 391–403; c) ADF 2008.01, SCM, Theoretical Chemistry, Vrije Universiteit, Amsterdam, The Netherlands, http://www.scm.com.
[16] a) C. Chang, M. Pelissier, M. Durand, *Phys. Scr.* **1986**, *34*, 394–404; b) E. van Lenthe, E. J. Baerends, J. G. Snijders, *J. Chem. Phys.* **1993**, *99*, 4597–4610; c) E. van Lenthe, E. J. Baerends, J. G. Snijders, *J. Chem. Phys.* **1994**, *101*, 9783–9792; d) E. van Lenthe, R. van Leeuwen, E. J. Baerends, J. G. Snijders, *Int. J. Quantum Chem.* **1996**, *57*, 281–293.
[17] a) K. Morokuma, *J. Chem. Phys.* **1971**, *55*, 1236–1244; b) T. Ziegler, A. Rauk, *Inorg. Chem.* **1979**, *18*, 1755–1759; c) T. Ziegler, A. Rauk, *Inorg. Chem.* **1979**, *18*, 1558–1565; d) G. Frenking, K. Wichmann, N. Fröhlich, C. Loschen, M. Lein, J. Lein, V. M. Rayon, *Coord. Chem. Rev.* **2003**, *238–239*, 55–82.
[18] F. Paulat, T. Kuschel, C. Nather, V. K. K. Praneeth, O. Sander, N. Lehnert, *Inorg. Chem.* **2004**, *43*, 6979–6994.

Received: August 25, 2010
Published Online: December 23, 2010

